HBM Tester Waveforms, Equivalent Circuits, and Socket Capacitance

Timothy J. Maloney
Intel Corporation, 2200 Mission College Blvd., SC9-09, Santa Clara, CA 95054 USA
tel.: 408-765-9389 e-mail: timothy.j.maloney@intel.com

Abstract - The Tektronix CT2 current probe is used to acquire more accurate Human Body Model waveforms with 0-ohm and 500 ohm tester loads than a CT1, owing to the CT2's low-frequency performance. The integrals and centroids of these waveforms then readily yield precise values of tester circuit elements and effective socket capacitance. Expressions are derived for effective socket capacitance resulting from distributed capacitance along a transmission line connecting to an unmatched load. These lead to options for reducing the effective socket capacitance while retaining the lines for delivering the HBM pulse.

I. Introduction

It was shown in 2009 [1] that HBM waveforms taken with a 0-ohm standard test load using a current probe can yield basic circuit modeling values for the tester, such as the charging capacitance C_{hb}, the time constant $R_{hb}C_{hb}$, and thus the series resistance R_{hb}. These parameters are extracted from "moments" of the waveform (integral and centroid, or 0^{th} and 1^{st} moments in this case) as described in [1], and extend from circuit analysis dating back to the Elmore theorem [2]. While obtaining C_{hb} from integrated current was fairly obvious, it was the Elmore theorem applied to the 2-pole RLC model of HBM that showed the ease of extracting true $R_{hb}C_{hb}$, irrespective of inductance L_1. While Ref. 1 cautioned that current measurements extracted with a CT1 current probe may have to be corrected for low frequency response of the probe, it is now found that the CT2 probe (also from Tektronix, Inc.) can provide good data for HBM tester characterization and circuit modeling, without significant need for correction.

The analytical methods of [1] can now be extended to a 4-pole model as used heavily for HBM work in the 1990s [3,4], to obtain circuit modeling information quickly and simply. As in [3], standard waveform measurements with loads of 0 and 500 ohms are used to deduce values of the parameters, notably C_{hb}, R_{hb} and socket capacitance C_2. C_{hb} and R_{hb} are the basic human body model parameters, of course, while socket capacitance needs to be limited because it produces extra stress on many ESD protection devices, stress that could be inappropriately destructive. This was well recognized in the 1990s and [3] presented electrothermal simulations showing the extent of that extra stress. Also, if a no-connect (NC) pin is stressed, the air will break down starting at about 800V and discharge the entire socket capacitance immediately, usually to a neighboring pin, producing an event far more destructive than HBM at the same voltage [5]. Ref. 3 also showed how difficult it was to achieve "selectivity" against high values of C_2 using only rise time and peak current standards with 0 and 500 ohms. To determine C_2 accurately seemed to require computer-driven multi-parameter analysis and curve fitting. In this work, we find that C_2 is far more accessible than we thought, through analysis of waveform moments. Highly "selective" methods for finding equivalent C_2 could be adopted if we wish, or at least we could quickly determine the C_2 of a tester that might produce a problem with a device during HBM testing.

II. Analytical Foundations

1. Extraction of s-domain Functions

The 2009 TLP and HBM waveform analysis work [1] discussed step response and continued with the insight of Elmore [2] and more recent authors [6,7], whereby it is shown that a waveform $h(t)$ is transformed into the Laplace domain by expanding the exponent in the transform as follows:

$$H(s) = \int_0^\infty h(t)e^{-st}dt$$

$$= \int_0^\infty h(t)[1 - st + \frac{s^2t^2}{2} - \frac{s^3t^3}{6} + \cdots]dt$$

$$= \sum_{k=0}^{\infty} \frac{(-1)^k}{k!} s^k \int_0^\infty t^k h(t)dt. \quad (1)$$

The various terms in the series are moments of the waveform, which yield coefficients of a Laplace domain function H(s) = $a_0+a_1s+a_2s^2+\ldots$ While an acceptable way of determining those coefficients, given a digital oscilloscope waveform *h*(t), would be to do the time integrals as in (1) (and discussed in [1] in terms of integration by parts), the Laplace transform formulation itself offers a more efficient and more easily implemented algorithm that was briefly treated in [1].

In this work, *h*(t) will be some kind of HBM waveform. Equation (1) tells us that the a_0 coefficient of H(s) is simply the integral *h*(t) from start to finish. But the Laplace treatment also tells us that this integral function $h_1(t) = \int_0^t h(\tau)d\tau$ transforms to $H_1(s) = H(s)/s = a_0/s+a_1+a_2s+\ldots$, as 1/s is the integration operator in the Laplace domain. Essentially, h_1(t) is a step of height a_0 with other features given by the rest of the coefficients. The Elmore Delay is indicated by a_1, after normalizing to a_0 and accounting for the (-1) factor. The next time-dependent function of interest thus subtracts the basic step height a_0 from h_1(t), i.e., $h_1'(t) = \int_0^t h(\tau)d\tau - a_0$ for which the transform is $H_1'(s) = a_1+a_2s+a_3s^2+\ldots$ We are back where we started with H(s), and know to find a_1 by integrating h_1'(t) to get h_2(t), then noting the step height again. The integral this time is the "area capture" integral as shown in [1], Fig. 9, and also later in this work, Fig. 6. Because we subtracted the step height to form h_1'(t), the integral is, strictly speaking, negative in our example, but that is expected from the (-1) factor for that term in Eq. 1, given a positive waveform. Thus the Elmore Delay ($-a_1/a_0$) is positive, as expected. With digital data and integration with (for example) a spreadsheet program, we can determine any and all coefficients through iteration as above. For many waveforms therefore, particularly a smooth one like HBM, the s-domain function H(s) is thus available, rather easily, to a number of coefficients (limited only by noise) and can be related to circuit models that predict those coefficients.

The above algorithm is very time-efficient on the computer if one is interested in a low-order polynomial, i.e., just the first few s-coefficients for acquiring circuit element knowledge. For N digital points in the scope waveform, the integral for each coefficient is of order N in time complexity, so for q coefficients, there are on the order of Nq operations (O(Nq)). In this work, we will find that q=2 applied to each waveform will be enough to determine our circuit elements. In contrast, using a fast Fourier transform (FFT) algorithm would have O(N*$\log_2$N) time complexity and would give N/2 frequency components, but this is far more information than needed for circuit modeling. The zero-frequency FFT component would correspond to a_0 but we would still have to take a derivative near zero frequency to find a_1. Even so, given that modern digital oscilloscopes usually offer quick FFT conversion of a waveform to the frequency domain, one may well want to use that FFT function to extract a_0 and a_1 (or more coefficients) quickly with a user-defined math function on the scope.

2. Transformers and Their Transfer Functions

Another aspect of the 2009 work [1] that we will use is the notion of a transfer function for transformers, such as the CT1 and CT2 current transformers for HBM that this paper discusses. As shown in [1], the low frequency cutoff of the transformer is an important property because it describes the "droop" experienced as the transformer tries to follow the HBM waveform out into the decay time of 150 ns and beyond. To a remarkable degree, for a given current level the step response of one of these transformers is an exponential decay, as in Figure 1, so a single pole can describe the transfer function for that aspect. Another pole can describe high frequency rolloff, in which case the complete transfer function for a current transformer like the CT1 or CT2 can be approximated, ignoring normalization factors, by

$$T(s) = \frac{s}{(s+a)(s+b)} \quad (2),$$

where $a=1/\tau_{xf}$, as in Fig. 1 and Ref. 1, and $b=1/\tau_{hf}$, indicating high frequency cutoff. Note that all transformers have a zero at zero frequency, thus the s in the numerator, but with that property, the step response is an easily observed exponential. As long as the frequency *b* is high enough to follow the rising edge of an HBM pulse well enough, our attention will

focus on the *a* frequency or τ_{xf}. τ_{xf} is current-dependent for both CT1 and CT2 probes, but while it is around 6.35 μsec for the CT1, it can be well over 100 μsec for the CT2. That will be significant.

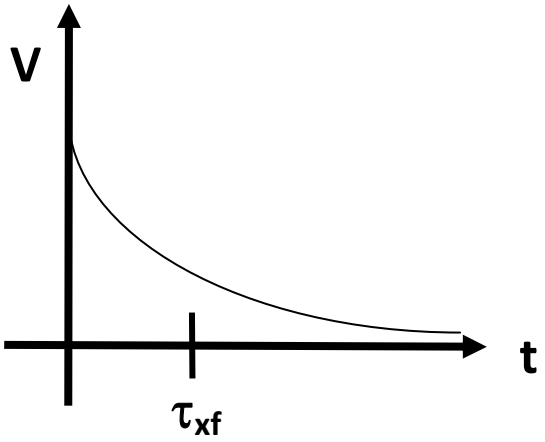

Figure 1. Step response of a transformer; τ_{xf} is the 1/e decay time.

With two poles, the step response of the transformer is a double exponential, with a fast rise time. The impulse response of the transformer is, as usual, the derivative of the step response, and it is the impulse response that gives us, through convolution [8], the observed HBM waveform. The near-delta function in the current probe's impulse response near t=0 will faithfully reproduce the HBM waveform, but it is the negative slope of the step response that gives us a weak or strong negative multiplier for the real HBM waveform in convolution. That is why a long τ_{xf} is desired for fidelity.

III. HBM Waveform Measurement

The Tektronix CT1 current probe [9] has traditionally been used for HBM waveform characterization [3]. Its high-frequency cutoff, approaching 1 GHz, is excellent for HBM rise times and peak currents, but its low-frequency cutoff is upwards of 100 kHz (Figure 2a) and causes noticeable sag in step response even at the 1 microsecond level [1]. Impulse response therefore has a strong negative component (imagine differentiating Fig. 1), and convolving such a response with the actual current waveform means that the decaying HBM current tail is depressed, and eventually drops below zero noticeably. This has surely caused systematic error in most measurements of HBM decay constant. Data taken with a CT1 can be corrected [1], but distortions are current-dependent [9], so it can be difficult to correct data accurately.

The Tektronix CT2 probe [9] has been found to be more suitable for HBM waveform measurement. Low-frequency cutoff is in the 1-10 kHz range (Figure 2b), which much better fits the HBM decay time of 150 nsec. Corrections are therefore negligible, and within electrical noise limits. This is indicated in Figure 3, comparing a section of the decay tail for the CT1 and CT2 probes on the very same pulse. The plunge below zero is clearly seen for the CT1. Meanwhile, rise time curves and peak current for 0 and 500 ohm loads are almost indistinguishable for CT2 versus CT1. In this case of a Thermo MK-4 tester, there was less than 1 per cent difference for those features, with 6-7 ns rise time for a 0 ohm load. The CT1 probe can always be used for rise time or peak current if there are any doubts about the CT2, but manufacturer data [9] indicates the impact of the CT2 bandwidth on those parameters may be negligible. At the same time, numerous measurements of the decay constant with the CT1 have shown that its droop, caused by low frequency response, is responsible for 0-ohm load decay constants failing the 130 ns minimum spec [11], particularly at 4kV, where distortion is greater. The CT2 then shows this "failure" to be a CT1 measurement artifact and not a tester fault. Use of the CT2 as the primary current probe for HBM waveforms is thus recommended.

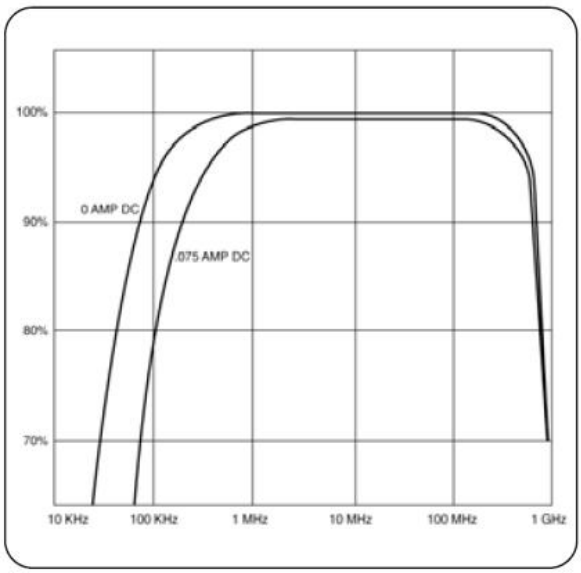

Figure 2a. Tektronix CT1 probe data, from [9].

IV. 4-pole HBM Model and Circuit Parameter Extraction

The traditional four-pole model (also called 4th order model) of HBM is shown in Figure 4, with elements

labeled as in [3]. One slight but important difference is the added voltage source, pictured as a step because we are indeed taking the circuit from charged C_{hb} to zero volts. We therefore are interested in the total admittance and response to a voltage step, giving the current.

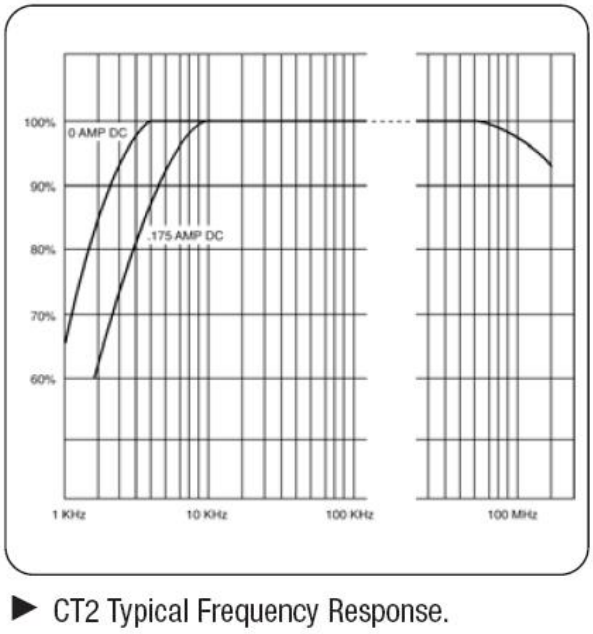

Figure 2b. Tektronix CT2 probe data, from [9].

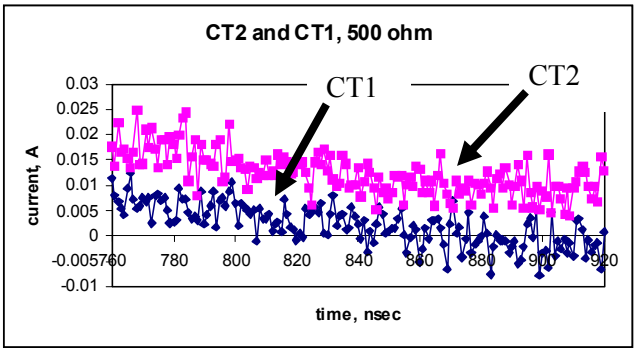

Figure 3. Expanded view of 500 ohm HBM tails for CT1 (lower) and CT2 (upper) current probes, with CT1 signal going negative because of its low frequency cutoff.

Approximate values of the circuit elements are as follows:

R_{hb} =1500 ohms

C_{hb} =100 pF

$C_1 \approx 2$ pF

$L_1 \approx 10$ µH

R_1 = 0 or 500 ohms

$C_2 \approx 20$ to 50 pF

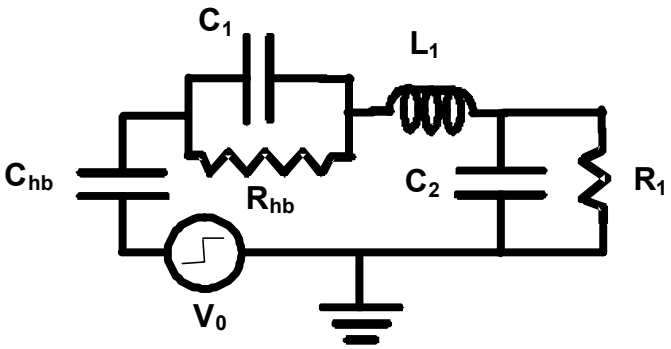

Figure 4. 4th order model of HBM ESD tester, including parasitic capacitances and inductance. As C_{hb} is initially charged to + or -V_0 and then discharges, HBM is conceptually the step response of this network.

It has long been recognized [3,4] that C_2 is the result of *distributed* capacitance, and therefore will depend on how R_1 compares to the effective Z of the transmission line. Ref. 3 found that 500 ohms was high enough to reveal nearly all of C_2. We discuss more about distributed capacitance in the next section.

The admittance functions for the circuit in Figure 4 can be written with standard methods in the Laplace domain, and reduced to expressions for the currents we can measure with a current probe in series with R_1, resembling some of the work done in [1]. The full admittance function in the s-domain for the 4-pole network is

$$Y(s) = \frac{C_{hb}s}{L_1 C_{hb}s^2 + \frac{R_{hb}C_{hb}}{1+R_{hb}C_1 s}s + \frac{R_1 C_{hb}}{1+R_1 C_2 s}s + 1} \quad (3)$$

The step voltage is $V=V_0/s$. For 0 ohms, C_2 drops out, the network is 3rd order, and we measure the full current as

$$I_0(s) = \frac{V_0 C_{hb}(1+R_{hb}C_1 s)}{1+b_{1-0}s+b_{2-0}s^2+b_{3-0}s^3}, \quad (4)$$

where $b_{1\text{-}0}=R_{hb}(C_{hb}+C_1)$, $b_{2\text{-}0}=L_1C_{hb}$, $b_{3\text{-}0}=L_1C_{hb}R_{hb}C_1$.

Full current is hard to measure for nonzero R_1, and is treated in Appendix A. For R_1=500 ohms, the current in the 500 ohm branch is

$$I_{500}(s) = \frac{V_0 C_{hb}(1+R_{hb}C_1 s)}{1+b_{1-500}s+b_{2-500}s^2+b_{3-500}s^3+b_{4-500}s^4}, \quad (5)$$

where $b_{1\text{-}500}=R_{hb}(C_{hb}+C_1)+R_1(C_{hb}+C_2)$,
$b_{2\text{-}500}=R_{hb}R_1(C_{hb}(C_2+C_1)+C_2C_1)+L_1C_{hb}$,
$b_{3\text{-}500}=L_1C_{hb}(R_{hb}C_1+R_1C_2)$, and

$b_{4\text{-}500}=L_1C_{hb}(R_{hb}C_1R_1C_2)$. In both cases the 0th order response is the total charge, $Q_t=V_0C_{hb}$. Figure 5 shows 0 and 500 ohm test load waveforms for a Thermo MK-4 tester with a CT2 probe, both revealing a capacitance C_{hb} of about 114 pF.

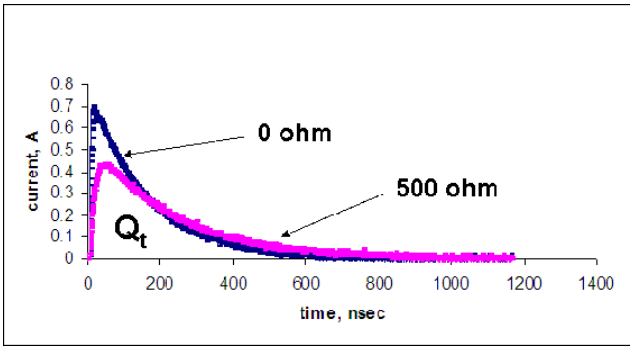

Figure 5. 0 and 500 ohm test load waveforms, 1kV, CT2 probe, measuring Q_t=114 nC in each case for an MK-4 tester.

Things get interesting as we investigate centroids of these waveforms, following the methods in [1] and as described in Section II above. In particular, [1] and Section II proved that the area A above the integrated current curve, divided by Q_t, gives the centroid of the original waveform (units of time), as shown in Figure 6. The centroids τ_0 and τ_{500} are of course the first-order s-coefficients (times -1) of the series expansions of the current expressions (4) and (5), again following [1]:

$$\tau_0 = b_{1-0} - R_{hb}C_1 = R_{hb}(C_{hb}+C_1) - R_{hb}C_1 = R_{hb}C_{hb}.$$
$$\tau_{500} = b_{1-500} - R_{hb}C_1$$
$$= R_{hb}(C_{hb}+C_1) + R_1(C_{hb}+C_2) - R_{hb}C_1$$
$$= R_{hb}C_{hb} + R_1(C_{hb}+C_2). \qquad (6)$$

Note that τ_0 is unchanged from the simple 2-pole model in [1]. In (5), let R_1 be the true value of the 500 ohm resistor, R_{500}. The socket capacitance C_2 therefore is

$$C_2 = \frac{\tau_{500} - \tau_0}{R_{500}} - C_{hb} \qquad (7)$$

Note that C_1 and L_1 have dropped out of the analysis and appear only in higher order moments. For the MK-4 tester discussed above, the complete set of extracted values is listed in Table I. The socket capacitance C_2=13.9 pF is considered a very good result, and indeed the waveforms easily passed all specs related to socket capacitance.

Tester	C_{hb}, pF	R_{hb}, kΩ	τ_0, nsec	τ_{500}, nsec	C_2, pF
MK-4	114	1.412	161	225	13.9
Zapmaster 512	101	1.445	146	222	51
Zapmaster 256	113.4	1.340	152	232.5	47.3

Table I. Major circuit model values and time constants for three different HBM testers at two different sites, using CT2 probe and 0 and 500 ohm (R_{500}=500-501 ohm) loads.

At the same time, older Zapmaster HBM testers, configured for 512 and 256 pins, at two different Intel sites, gave R_{hb} and C_{hb} values as shown (see Table I), but with higher socket capacitance C_2=47-51 pF. Sure enough, in the 512 case the 500 ohm Ipeak value did not pass spec. The 0-ohm load decay for the 512 was short enough that it failed on a CT1 probe (128 ns) but passed on a CT2 (135 ns). The 256 waveforms narrowly passed specs on the CT1 but had much healthier margins on the CT2. All this is in agreement with the notion that JEDEC and ESDA HBM specs were formulated with the intention of tolerating up to 50 pF of equivalent socket capacitance.

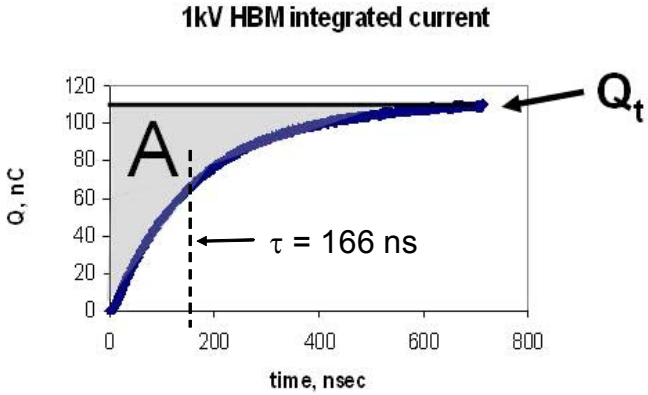

Figure 6. Integrated current for a 1 kV HBM waveform, converging to total charge Q_t. The centroid τ of the original waveform is computed from $A/Q_t = \tau$, where A is the area above the curve, and is the Elmore Delay of this integrated current curve. Related theorems are proven in [1].

V. Distributed Socket Capacitance

An automated HBM ESD tester acquires much of its apparent inductance L_1 and socket capacitance C_2 from the distributed transmission lines through the relays to the socket board. That portion of the lumped element model as in Fig. 4 can be found from a first order approximation of the transmission line model, terminated by resistance R_1 (0 and 500 ohms) with line impedance $Z_0=1/Y_0$. This is illustrated in Figure

7, for which we want to find a simple network equivalent of Z_{in} or Y_{in}. For R_1=0, there will be some L_1 and no C_2, but from Eqs. 1-7, it is clear that L_1 does not affect the first-order C_2 calculation that we arrive at in Eq. 7 once we have a lumped model. Thus we turn to the case of R_1=500 ohms and look at the input admittance, aiming for $Y_{in} = \frac{1}{R_1} + j\omega C_x = Y_1 + sC_x$

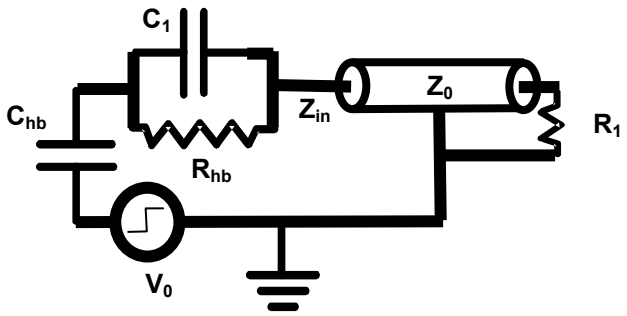

Figure 7. HBM circuit model with distributed inductance and capacitance (L_1 and C_2 as in Fig. 4) shown as a transmission line from the HBM network module to the socket load R_1. Z_{in} (equal to $1/Y_{in}$) is expected to yield equivalent C_2.

and effective capacitance C_x. From transmission line theory [10],

$$Y_{in} = Y_0\left[\frac{Y_1 + Y_0 \tanh\gamma\ell}{Y_0 + Y_1 \tanh\gamma\ell}\right] \approx \frac{Y_1 + sY_0\sqrt{LC}\,\ell}{1 + s\frac{Y_0}{Y_1}\sqrt{LC}\,\ell}\ , \quad (8)$$

for low values of $\gamma\ell$, γ the propagation constant $j\omega\sqrt{LC}=s\sqrt{LC}$, L and C the capacitance and inductance of the line per unit length, and ℓ the line length. Also $Y_0^2=C/L$ for the lossless transmission line. To first order, the denominator expands for low values of $\gamma\ell$ to multiply the numerator, resulting in

$$Y_{in} = Y_1 + s\frac{Y_0^2 - Y_1^2}{Y_0}\sqrt{LC}\,\ell + \cdots \quad (9)$$

If the full distributed capacitance is $C_2=C\ell$, this becomes

$$Y_{in} \approx \frac{1}{R_1} + sC_2\left(1 - \frac{Z_0^2}{R_1^2}\right) = \frac{1}{R_1} + s\alpha C_2. \quad (10)$$

As expected, the effective capacitance $C_x=\alpha C_2$ declines with higher Z_0 and tunes out completely with an impedance match of $R_1=Z_0$. This means that one strategy for reducing C_x is to raise the effective Z_0, say by distributing nearly lossless "loading coils" (e.g., ferrite beads) along the line. This recalls a coil loading method used in the 19th century to reduce the resistive attenuation of telegraph signals, as the attenuation length is approximately $2Z_0/R$, R the resistance per unit length [10], although the purpose here is slightly different. The extra total inductance puts some limits on the shortest achievable HBM rise time (see Appendix A), but the 2-10 ns window for 0-ohm loads [11], for example, should not be threatened by a few extra microhenries.

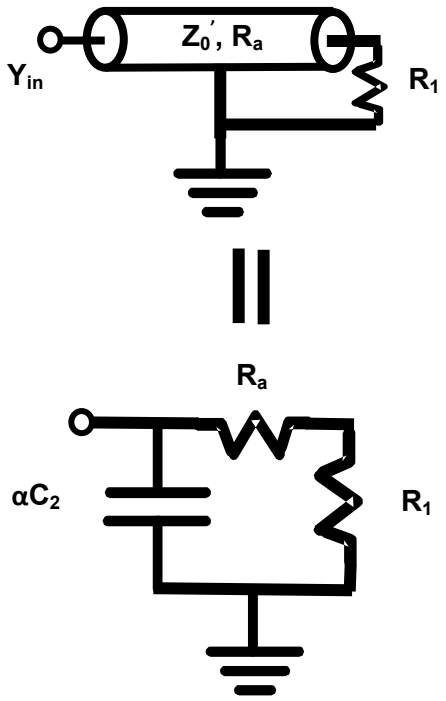

Figure 8. Expressions for the Y_{in} of the distributed section of the HBM model with total distributed resistance R_a give an equivalent socket capacitance αC_2 and parallel resistance as shown. Eq. (16) is the general expression for the socket capacitance reduction factor α. The HBM network module resistance R_{hb} should be reduced by (approximately) R_a in order to preserve the waveform properties as discussed in Section IV.

Another way to reduce C_x is to borrow from the HBM network's 1500 ohms of series resistance and distribute some resistance R_a along the transmission lines that also have their distributed capacitance totaling C_2. If the inductance now becomes negligible, $\gamma\ell = \sqrt{R_a C_2 s}$, $Z_0 = \sqrt{\frac{R_a}{sC_2}}$, and

$$Z_{in} = Z_0\left[\frac{1 + \frac{Z_0}{R_1}\tanh\gamma\ell}{\frac{Z_0}{R_1} + \tanh\gamma\ell}\right]$$

$$= Z_0 \tanh \gamma\ell \left[\frac{1 + \frac{Z_0 \tanh \gamma\ell}{R_1}}{\frac{Z_0 \tanh \gamma\ell}{R_1} + \tanh^2 \gamma\ell} \right]. \quad (11)$$

But for small $\gamma\ell$, $\tanh\gamma\ell \approx \gamma\ell$, $Z_0\gamma\ell = R_a$, and

$$Z_{in} \approx R_a \left[\frac{1 + \frac{R_a}{R_1}}{\frac{R_a}{R_1} + sR_aC_2} \right] = \frac{1 + \frac{R_a}{R_1}}{\frac{1}{R_1} + sC_2}. \quad (12)$$

This means that

$$Y_{in} \approx \frac{1}{R_1 + R_a} + s\alpha C_2, \quad (13)$$

where $\alpha = R_1/(R_a+R_1)$, and corresponds to the circuit model in Figure 8. The effective capacitance $C_x = \alpha C_2$ and is reduced accordingly by the distributed resistance R_a. But if the total inductance L_t is <u>not</u> negligible, R_a is simply replaced by R_a+sL_t ($=Z_0\gamma\ell$) in (12-13), leading us to a more general expression

$$Y_{in} = \left[\frac{1}{R_1} + sC_2 \right] \left[\frac{R_1}{R_a + R_1} \left(\frac{1}{1 + \frac{Z_0'^2 C_2 s}{R_a + R_1}} \right) \right]. \quad (14)$$

We now take $Z_0' = \sqrt{\frac{L_t}{C_2}}$ for the transmission line, while the actual impedance is complex and includes the effect of R_a. Expanding this to first order, we have

$$Y_{in} \approx \frac{1}{R_1 + R_a} + sC_2 \left[\frac{R_1}{R_a + R_1} \left(1 - \frac{Z_0'^2}{R_1(R_a + R_1)} \right) \right]. \quad (15)$$

This reduces to (10) for $R_a=0$ and to (13) for L_t or Z_0' negligible, so now we see that the general capacitance reduction factor is

$$\alpha = \frac{R_1}{R_a + R_1} \left(1 - \frac{Z_0'^2}{R_1(R_a + R_1)} \right) \quad (16)$$

for a transmission line with inductive and resistive loading as above. From this expression, it can be easily shown that the tradeoff of R_a and Z_0' is particularly simple when $\alpha<0.5$ is desired, as that condition is

$$R_a^2 + 2Z_0'^2 > R_1^2. \quad (17)$$

Therefore when $R_1=500$ ohms, $\alpha<0.5$ is achieved with 300 ohms for each of R_a and Z_0', for example, along with other solutions beyond the elliptical boundary in the R_a- Z_0' plane. Lower effective capacitance of this kind also has the desired effect on sudden destructive currents that can be delivered in snapback [3] or in breakdown of a no-connect pulse [5], as the inductive and resistive loading limits the current.

VI. Conclusions

The Tektronix CT2 current probe is found to be adequate for short-time HBM waveform measurements like rise time and peak current, and more suitable than the same manufacturer's CT1 probe for long-time measurements like decay constant. CT2 waveforms do not suffer from significant droop in HBM waveform tails, making them suitable for circuit element extraction through asymptotic waveform analysis methods, even with a 4-pole model of HBM.

Integration of the 0-ohm load waveform gives main HBM capacitance C_{hb}, and the waveform's first moment or centroid gives the $R_{hb}C_{hb}$ time constant τ_0 and therefore R_{hb}, through straightforward and essentially graphical means. While the authors of Ref. 3 found that only a careful multi-parameter fit to waveforms could determine a best value of C_2, the methods here, summarized by Eq. 7, allow tester equivalent socket capacitance C_2 to be accurately measured from the 0-ohm values (C_{hb}, τ_0) plus the 500 ohm centroid time constant. This allows a precise measurement of this important value with a simple, easily accessible method, as the error in C_2 should be limited only by noise and numerical accuracy. The method leading up to Eq. 7 provides the "selectivity" for C_2 that has long been sought by ESD researchers. A related qualification standard would depend on acceptance of digital waveform records and procedures for extracting simple integrals and centroids from the waveforms.

Much of the effective socket capacitance αC_2 in an HBM tester can result from the necessarily long distribution lines from the HBM network module to the component at the socket. The network analysis methods of this paper are extended to find the effective socket capacitance that results from (1) the known finite impedance and terminating load of the transmission line, and (2) distributing some of the required 1500 ohms of series resistance throughout this transmission line. Simple general expressions for αC_2 then show how inductive loading and/or distributed series resistance can substantially reduce

this capacitance and thus reduce unwanted extra stress during the HBM test. Newer HBM testers have much lower αC_2 and are already using these methods.

Appendix A: Additional Mathematics

For nonzero R_1, the full current is found from Eq. 3 to be

$$I_{full-500}(s) = \frac{V_0 C_{hb}(1+R_{hb}C_1 s)(1+R_1 C_2 s)}{1+b_{1-500}s+b_{2-500}s^2+b_{3-500}s^3+b_{4-500}s^4}. \quad \text{(A1)}$$

This is Eq. 5 with one more zero. Thus the measured $I_{500}(t)$ is the convolution of $I_{full\text{-}500}(t)$ with $\exp(-t/R_1C_2)$, so for a fast rise time on $I_{full\text{-}500}(t)$, the R_1C_2 time constant is expected to add to it and dominate the rise time of $I_{500}(t)$. HBM test standards [11] have agreed with this.

Note that all these network functions are ratios of polynomials. The essential properties of the functions can be examined by considering each network function to be

$$H(s) = \frac{1+a_1 s+a_2 s^2+\cdots+a_n s^n}{1+b_1 s+b_2 s^2+\cdots+b_m s^m}, \quad \text{(A2)}$$

$m \geq n$, and corresponding to time domain function $h(t)$. It is useful to expand $H(s)$ about s=0 to obtain an infinite series in powers of s,

$$H(s) = 1+(a_1-b_1)s+(a_2-b_2-b_1a_1+b_1^2)s^2 + (a_3-b_3-a_1b_2+2b_1b_2-a_2b_1+a_1b_1^2-b_1^3)s^3+\cdots \quad \text{(A3)}$$

This kind of result appears in many works on signal integrity [6]. It is also useful to consider the factors of the numerator and denominator of $H(s)$, described by the m poles p_i and the n zeros z_i that form the roots of the polynomials. It is a consequence of Vieta's Formulas describing the relations among symmetric polynomials S_q [12] of these roots to the coefficients that we can form S_{n-1}/S_n for the poles and zeros and find that

$$\sum_{i=1}^{m}\frac{1}{p_i} = -b_1, \sum_{i=1}^{n}\frac{1}{z_i} = -a_1. \quad \text{(A4)}$$

Remember that the real parts of our poles and zeros will typically be negative numbers, and the coefficients positive real, so the minus signs can be dropped if we regard the reciprocal poles and zeros as positive time constants. Note also that complex conjugate poles or zeros $\sigma \pm j\omega$ add together to become a real number $2\sigma/(\sigma^2+\omega^2)$.

The fact that the poles and zeros sum to an easily calculated number can be used to refine some of our estimates. In the 1993 work by Verhaege, et al., [3], the main decay constant τ_2 for the 4th order network is found to be

$$\tau_2 = (R_{hb}+R_1)(C_{hb}+C_1). \quad \text{(A5)}$$

For the shorting waveform $R_1=0$, this reduces to

$$\tau_{20} = R_{hb}(C_{hb}+C_1). \quad \text{(A6)}$$

However, in the expression for $I_0(s)$, Eq. 4, this corresponds to $b_{1\text{-}0}$, the sum of <u>all</u> the poles, including rise time plus decay constant. It is clearly correct for $L_1=0$, where everything collapses to a single pole, but then the rise time would be zero and out of spec. Some influence of inductance is expected, as is the case for a 2-pole network (note that $1/a + 1/b = R_{hb}C_{hb}$). By starting with $L_1=R_1=0$ and adding in L_1 as a "small" perturbation, one gets

$$\tau_{20} \approx R_{hb}(C_{hb}+C_1) - \frac{L_1}{R_{hb}}\left(1-\frac{2C_1}{C_{hb}}+\frac{L_1 C_{hb}}{R_{hb}^2(C_{hb}+C_1)^2}\right) \quad \text{(A7)}$$

The last term indicates the rise time of the HBM network, with the expected L/R leading term.

Acknowledgements

The author would like to thank Russell Sears, Marti Farris and Abishai Daniel of Intel for the HBM tester data, acquired using both CT1 and CT2 current probes. Thanks also to Evan Grund for manuscript review and additional insights.

References

[1] Timothy J. Maloney, "Evaluating TLP Transients and HBM Waveforms", EOS/ESD Symposium Proceedings, pp. 143-151, 2009.

[2] W.C. Elmore, "The Transient Analysis of Damped Linear Networks With Particular Regard to Wideband Amplifiers", J. Appl. Phys. Vol. 19(1), pp. 55-63 (1948).

[3] K. Verhaege, P. Roussel, G. Groeseneken, H. Maes, H. Gieser, C. Russ, P. Egger, X. Guggenmos, and F. Kuper, "Analysis of HBM ESD Testers and Specifications Using a 4th Order Lumped Element Model", EOS/ESD Symposium Proceedings, pp. 129-137, 1993.

[4] L. van Roozendaal, A. Amerasekera, P. Bos, W. Baelde, F. Bontekoe, P. Kersten, E. Korma, P. Rommers, P. Krys, U. Weber and P. Ashby, "Standard ESD Testing of Integrated Circuits",

EOS/ESD Symposium Proceedings, pp. 119-130, 1990.

[5] H. Kunz, C. Duvvury, J. Brodsky, P. Chakraborty, A. Jahanzeb, S. Marum, L. Ting, and J. Schichl, "HBM Stress of No-Connect IC Pins and Subsequent Arc-Over Events that Lead to Human-Metal-Discharge-Like Events into Unstressed Neighbor Pins", EOS/ESD Symposium Proceedings, pp. 24-31, 2006.

[6] R. Gupta, B. Tutuianu, and L.T. Pileggi, "The Elmore Delay as a Bound for RC Trees with Generalized Input Signals", IEEE Trans. on Computer-Aided Design of Integrated Circuits and Systems, vol 16, no. 1, pp. 95-104, January 1997.

[7] M. Celik, L. Pileggi, and A. Odabasioglu, *IC Interconnect Analysis*, (New York: Kluwer Academic Publishers, 2002).

[8] R.N. Bracewell, *The Fourier Transform and Its Applications*, (New York: McGraw-Hill, 1965).

[9] Web article, Tektronix page on CT1, CT2, and CT6 current probes: http://www2.tek.com/cmswpt/psdetails.lotr?ct=PS&lc=EN&ci=13500&cs=psu. Figs. 2a, 2b used with permission.

[10] S. Ramo, J. Whinnery, and T. Van Duzer, *Fields and Waves in Communication Electronics,* (New York: John Wiley & Sons, 1965), p. 46.

[11] ANSI/ESDA/JEDEC JS-001-2010, ESDA/JEDEC Joint Standard for Electrostatic Discharge Sensitivity Testing--Human Body Model (HBM)--Component Level (Jan. 2010). Available at www.jedec.org and www.esda.org.

[12] Web articles, http://mathworld.wolfram.com/PolynomialRoots.html, also http://mathworld.wolfram.com/VietasFormulas.html.